Simple Energy Landscape Model for the Kinetics of Functional Transitions in Proteins

Osamu Miyashita,[†] Peter G. Wolynes,[†,‡] and José N. Onuchic*[,†]

Center for Theoretical Biological Physics and Department of Physics and Department of Chemistry and Biochemistry, University of California at San Diego, 9500 Gilman Drive, La Jolla, California 92093

Received: July 22, 2004; In Final Form: November 5, 2004

It is evident that protein conformational transitions play important roles in biological machinery; however, detailed pictures of these transition processes capable of making kinetic prediction are not yet available. For a full description of these transitions, we first need to describe kinematically movements between stable states. Then, more importantly, a free energy profile associated with the conformational change needs to be obtained. Recently, a new model to describe the energy landscape of protein conformational changes was applied to the conformational transition of adenylate kinase [Miyashita, O.; Onuchic, J. N.; Wolynes, P. G. *Proc. Natl. Acad. Sci. U.S.A.* **2003**, *100*, 12570−12575]. In this model, the conformational change coupled to the ligand binding is described as a switching between two energy surfaces that correspond to ligand bound and unbound states. The nonlinearity of the protein conformational changes is described through an iterative usage of normal mode calculations. In addition, another kind of nonlinearity enters the dynamics of the conformational transitions due to cracking, or partial unfolding, which may occur during the conformational transitions. The consequences of this theoretical model are explored in greater detail. An improved model for the cracking that includes the cooperativity of the partial unfolding in analogy to nucleation is introduced.

Introduction

Proteins often undergo large conformational changes upon ligand binding. It is evident that such conformational transitions play important roles in the machinery of the cell. Nevertheless, the details of these transition processes are not yet fully understood. Such functional transitions require a biomolecule to have at least a pair or, more likely, a multiplicity of conformational states of nearly equal free energy. For a full description of these transitions, we first need to describe movement between such states. Then, more importantly, the energy landscape associated with the conformational change need to be obtained.

Several methods have been developed to describe the conformational transitions of the proteins. The simplest way to obtain the conformational change path is an interpolation of the two end-state structures followed by energy minimization[1] or an interpolation in internal coordinates.[2] These methods are useful to obtain a qualitative picture of the conformation change. However, they do not provide energetics. Other approaches use molecular dynamics simulation with biasing potentials to force the protein to move from one conformation to the other.[3,4] These methods have limitations due to the complexity of the model because molecular dynamics simulations are often too time-consuming to be applied to large-scale conformational changes. Using a strong biasing potential to overcome the time scale problem may result in the generation of unrealistic conformational changes. Alternative methods are based on normal-mode analysis. Large-scale protein motions are often parallel to the low-frequency normal modes.[5,6] Even in its simplest form, the notion of normal modes has been remarkably successful for visualizing and predicting the character of the protein conformational change pathways.[7−9] Yet, clearly, a linear normal mode description cannot be completely accurate because considerable anharmonicity resides in protein dynamics. The normal mode picture describes the excitations around a single minimum. This limited adequacy of the normal mode description becomes even more apparent when we try to discuss energetics of motions between dominant conformational states with different energy minimum conformations.

We recently developed a model to describe the energy landscape of protein conformational changes, which was applied to the conformational transition of adenylate kinase.[10] In this model, in analogy to the theory of electron-transfer reactions,[11,12] two energy surfaces that correspond to different states of the protein, such as ligand bound and unbound states, are considered. Structural deformation between the open and closed forms occurs via low-frequency modes on separate reactant and product surfaces, with a switching between the two different energy surfaces at their crossing region. The nonlinearity of the protein conformational changes is described through an iterative use of normal mode calculations. The energy barrier of the conformational change that arises from this procedure, however, is very large; it is larger than the energy needed to fully unfold the protein. Therefore, we proposed a *cracking* mechanism, i.e., proteins locally unfold in regions of large elastic stress during conformational transitions. Unlike macroscopic machines, biological machines can locally break and then reassemble during their function. Cracking leads to a counterintuitive catalytic effect of added denaturant on allosteric enzyme function.

In the present work, we revisit the previously proposed model and make several improvements in the model. The analogy between our model for the protein conformational transition and the electron transfer theory is discussed more fully. We attempt to estimate the energy barrier of the conformational change of

* Corresponding author: e-mail jonuchic@ucsd.edu.
† Center for Theoretical Biological Physics and Department of Physics.
‡ Department of Chemistry and Biochemistry.

10.1021/jp046736q CCC: $30.25
Published on Web 01/13/2005

the adenylate kinase through a pure normal mode model, on which formalisms of electron transfer theory is exact. From this, it becomes evident that the description of protein conformational transition requires to go beyond the simple normal mode picture. However, still, the analogy to the electron transfer theory raises some interesting questions for studies of conformational transitions, such as dependence of the kinetic rate of the conformational change on driving force. In addition, we discuss more details of the conformational change of the adenylate kinase, using polar rotation angles of mobile domains as reaction coordinates, instead of RMSD. With this new reaction coordinate, the switching between the energy surfaces can be described more precisely. Finally, a new model for the cracking, or the partial unfolding, is discussed in which the cooperative aspect of partial unfolding is described by a new scheme in analogy to a nucleation process.

Theory and Models

In the simplest case of allosteric conformational change, the system involves two dominant conformational states. Conformational changes such as domain closure often occur upon ligand binding. While a widely believed model of the domain closure is that the ligand binds first and then stabilizes the closed conformation, this assumption is open to debate. If the ligand binding occurs concurrently with the structural transformation, then the situation becomes substantially more complex. First, two energy landscapes each corresponding to the two states of ligand being bound and not being bound need to be considered to describe such ligand-induced conformational changes. For the energy state before the ligand binding, i.e., ligand-unbound state, the open form is the most stable form of the protein. In the same way, the closed form corresponds with the ligand-bound state. Nevertheless, even for the situation where no ligand is bound, the closed form can be partially stable.[13] Thus, in general, two energy minima coexist for each of the ligand-binding states, i.e., four energy surfaces in total are necessary to discuss the entire binding and rearrangement process. In this work, as a starting point, we will consider only two energy surfaces: the ligand-unbound state with the open form as an energy minimum and the ligand-bound state with the closed form as an energy minimum. The ligand-induced conformational change is assumed to occur by switching from one state to another upon ligand binding. A general scheme of the ligand binding coupled conformational change would allow ligand binding and unbinding at any conformation of the protein:

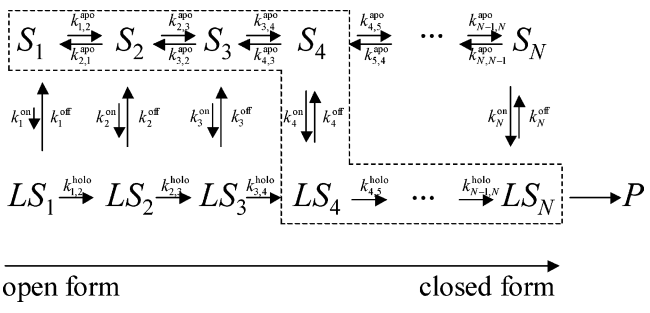

where N is the number of representative conformations of the protein, S_i is the conformation i, and LS_i is the same protein conformation with the ligand bound. The S_1 is the open form, which is most stable without the ligand, and the LS_N is the closed form, which is the most stable conformation with the ligand being bound. P is the product state, resulting from the ligand bound stable form, LS_N. We assume that $E_i^{\mathrm{unbound}} < E_{i+1}^{\mathrm{unbound}}$, where E_i^{unbound} is the unbound state energy (the sum of protein and ligand) of the conformation, i. We also assume that $E_i^{\mathrm{bound}} > E_{i+1}^{\mathrm{bound}}$, where E_i^{bound} is the bound state energy of the conformation, i. The zero points of the energies are set $E_1^{\mathrm{unbound}} = 0$ and $E_N^{\mathrm{bound}} = 0$.

The binding of the ligand to the protein would be stronger when the conformation is closer to the closed form; thus $k_i^{\mathrm{on}}/k_i^{\mathrm{off}} < k_{i+1}^{\mathrm{on}}/k_{i+1}^{\mathrm{off}}$. If the rates of conformational transitions, $k_{i,j}^{\mathrm{apo}}$, are slower than the rate of the ligand binding processes, the representative binding processes would occur at a conformation, i, where the binding process becomes substantial compared to the unbinding process, $k_i^{\mathrm{on}}[L] \sim k_i^{\mathrm{off}}$, where $[L]$ is the concentration of the ligand in molar. If we assume $k_i^{\mathrm{on}}/k_i^{\mathrm{off}} = A \exp[-(E_i^{\mathrm{bound}} - E_i^{\mathrm{unbound}})/k_{\mathrm{B}}T]$, where A is a constant to be determined, the last condition gives

$$E_i^{\mathrm{unbound}} - E_i^{\mathrm{bound}} + k_{\mathrm{B}}T \log [L] + k_{\mathrm{B}}T \log A = 0$$

where k_{B} is the Boltzmann constant and T is the temperature.

To obtain the constant, A, we consider the system at equilibrium with concentrations, $[\bar{S}_i]$, $[\overline{LS_i}]$, and $[\bar{L}]$. For the conformation that satisfies the above resonance condition (i = TS), the binding−unbinding process should be at equilibrium; thus, $k_{\mathrm{TS}}^{\mathrm{on}}[\bar{S}_{\mathrm{TS}}][\bar{L}] = k_{\mathrm{TS}}^{\mathrm{off}}[\overline{LS_{\mathrm{TS}}}]$. Using $[\bar{S}_{\mathrm{TS}}] = \exp(-E_{\mathrm{TS}}^{\mathrm{unbound}}/k_{\mathrm{B}}T)[\bar{S}_1]$ and $[\overline{LS_{\mathrm{TS}}}] = \exp(-E_{\mathrm{TS}}^{\mathrm{bound}}/k_{\mathrm{B}}T)[\overline{LS_N}]$, we obtain

$$\frac{k_{\mathrm{TS}}^{\mathrm{on}}}{k_{\mathrm{TS}}^{\mathrm{off}}} = \mathrm{e}^{-(E_{\mathrm{TS}}^{\mathrm{bound}} - E_{\mathrm{TS}}^{\mathrm{unbound}})/k_{\mathrm{B}}T} \frac{[\overline{LS_N}]}{[\bar{S}_1][\bar{L}]}$$

Thus, the constant $A = [\overline{LS_N}]/[\bar{S}_1][\bar{L}] \sim 1/K_{\mathrm{D}}$, where K_{D} is the dissociation constant. Finally, the resonance condition is

$$E_i^{\mathrm{bound}} + \Delta G^\circ - k_{\mathrm{B}}T \log[L] - E_i^{\mathrm{unbound}} = 0 \qquad (1)$$

where ΔG° is the standard reaction free energy of this binding process. Thus, the binding process occurs at the intersection region of the free energy surfaces of the ligand-bound state and the ligand-unbound state. Note that under this scheme the free energy drive for the reaction would be ligand concentration dependent, while under the assumption of slow binding and release, the free energy drive will not depend on the ligand concentration. In both limiting cases, consideration of only two surfaces is necessary for the analysis of the rearrangement kinetics. The present model could be generalized by considering the binding events occurring at the vicinity of the intersection region, as in the Agmon−Hopfield model.[14]

Linear Elastic Model To Estimate the Energy Barrier. When the energy surface of each of the two states of conformational change can be approximated as quadratic functions of the coordinates, the dynamics on each surface can be described by normal-mode analysis.[15] Under this approximation, the energy barrier can be estimated by normal-mode analysis. The energy surface of the ligand-unbound state is described by normal modes as

$$E_{\mathrm{unbound}} = \sum_n \frac{1}{2} \omega_n^2 q_n^2$$

where ω_n is the frequency of mode n and q_n is the normal mode coordinate of mode n. If perturbation to the energy due to the ligand binding is small and the normal modes of two states are the same, we can describe the energy of the final state as

$$E_{\text{bound}} = \sum_n \frac{1}{2}\omega_n{}^2 q_n{}^2 + \sum_n c_n q_n$$

In the harmonic regime, in the same way as the theory of the electron-transfer reactions, the activation free energy, ΔG^*, can be expressed as[12]

$$\Delta G^* = \frac{(\lambda + \Delta G)^2}{4\lambda} \tag{2}$$

where ΔG is the reaction free energy and λ is the reorganization energy (see Figure 1a for the definition). Using the normal mode variables, the reorganization energy can be obtained as[16]

$$\lambda = \sum_n \lambda_n = \sum_n \frac{1}{2}\omega_n{}^2 \Delta q_n{}^2 \tag{3}$$

where Δq_n is the difference of two minima in normal mode coordinate of mode n, i.e., $\Delta q_n = c_n/\omega_n{}^2$. From these relations, it is evident that the conformation can change more by motion along a lower frequency mode at the same cost of energy. This explains the observation that large-scale protein conformational changes are very close in form to the lowest frequency modes.[6] The total reorganization energy, λ, is obtained as the sum of contributions from each normal mode, λ_n. This model involves two kinds of linearity: first, structural deformations are approximated linearly as being along a normal mode vector, and second, the energy gap is approximated as a linear function of the coordinate. Both of these assumptions are consequences of the harmonic approximation of the energy surface as a function of atomic coordinates. We call this formalism "the linear elastic model".

Energy Surface of Conformational Change Described by the Nonlinear Elastic Model. The linear elastic model gives a rough estimate of the energy barrier and a qualitative picture of the energy surface of conformational change. Nevertheless, this model has some limitations owing to the linearity approximations (see Results). The actual energy surface is not simple harmonic, and the conformational change cannot be described by a linear normal mode picture. Kinematic nonlinearity of the conformational change can be described by an iterative procedure.[10] In the iterative procedure, the structure is slightly deformed along a few normal modes that are most relevant to the conformational change, and the normal modes are recalculated repeatedly as structure changes. In this way, it is the strains that are assumed to be small, not the total displacements. The number of normal modes used at each iteration step affects the conformational change path. We use the same parameters as in our previous study,[10] except that we limit the maximum displacement (RMSD) to 0.1 Å in this study. For each of the ligand-unbound and -bound states, energy surfaces along nonlinear conformational change paths are generated. From superposition of the energy surfaces, the energy barrier of the conformational transition is obtained.

Cracking Model. The energy barrier that arises from the above procedure is very large, even when the kinematic nonlinearity of the conformational change is taken into account. It is larger than the energy needed to fully unfold the protein. In our previous study, we observed that the strain energy is localized in the molecule, and only some particular residues are under high strain. This observation led us to hypothesize that these highly strained residues *crack*, i.e., unfold partially, during conformational change.[10] To include this possibility, we consider a model where residues are allowed to partially unfold if their strain energy is higher than a certain threshold, which is the difference between the local folding energy and the entropy to be gained by local unfold. Under this approximation, each of the residues can have two states, "folded state" or "unfolded state", and the free energy per residue can be written as

$$G^{\text{residue}} = \begin{cases} E_0^{\text{residue}} + E_{\text{strain}}^{\text{residue}} & \text{when the residue is folded} \\ -TS^{\text{residue}} & \text{when the residue becomes unfolded} \end{cases} \tag{4}$$

We make the approximation that all residues have identical contact energy, E_0^{residue}, at the initial state and that the entropy change upon unfolding, S^{residue}, is also the same for all residues. Though it is easy to incorporate residue specific energies for the threshold as in the work of Munoz and Eaton,[17] we keep uniform values for simplicity only. We assume that the unfolding energy of one residue is equal to the total unfolding energy divided by the number of residues. Thus, the threshold of the cracking, $\Delta G^{\text{residue}} = -TS^{\text{residue}} - E_0^{\text{residue}}$, is assigned to $\Delta G_{\text{fold}}/N_{\text{res}}$, where ΔG_{fold} is the total stability of the protein and N_{res} is the number of residues. The threshold of the ligand bound state, $\Delta G_{\text{bound}}^{\text{residue}}$, is related to the threshold of the ligand unbound state, $\Delta G_{\text{unbound}}^{\text{residue}}$, in such a way that the bound and the unbound states have the same energy when they are completely unfolded, i.e., $N_{\text{res}}\Delta G_{\text{unbound}}^{\text{residue}} - N_{\text{res}}\Delta G_{\text{bound}}^{\text{residue}} = \Delta G_{\text{react}}$, where ΔG_{react} is the free energy difference between the ligand-unbound and -bound states. In addition, we need to consider the cooperative aspect of denaturation. Cooperativity implies there is another condition for cracking involving the size of region that is under high strain. Partial unfolding would occur only when several contiguous residues are simultaneously under high strain to unfold. In our previous study, we allowed the cracking to occur only if more than five residues along the sequence are under high strain. In the present work, we model cooperativity in analogy to a nucleation process. We assume that the crack induces a surface cost, σ, at the boundary of folded and unfolded regions. Thus, in addition to the previous condition, the total stabilization gain from crack formation must be larger than 2σ to allow the cracking of a region. The modified model renders many of our discussions more transparent, since the surface cost is now the only adjustable parameter.

In the present study, we also assume that the binding process is fast and the unfolded regions remain unfolded during the switching between the two energy surfaces. We now consider the conformational transition path from the ligand-unbound state to the bound state. For each structure, the residue energy of the ligand-unbound state, $G_{\text{unbound}}^{\text{residue}}$, is obtained through the above cracking model. If the cracking condition is met, the residue is unfolded. These unfolded residues remain unfolded even after the switching to the bound state. Thus, the residue energy of the bound state, $G_{\text{bound}}^{\text{residue}}$, is equal to that of the unfolded state, $-TS^{\text{residue}}$(no matter how much strain energy the residue has in the bound state). For the residues that were folded in the unbound state, $G_{\text{bound}}^{\text{residue}}$ is the strain energy of the bound state. They remain folded even if the strain energy is higher than the threshold, $\Delta G_{\text{bound}}^{\text{residue}}$. The strain energy of the bound state is calculated using the closed form as the stable reference conformation.

Method

Studied System. In this study, we illustrate the ideas using adenylate kinase. Adenylate kinase catalyzes the interconversion

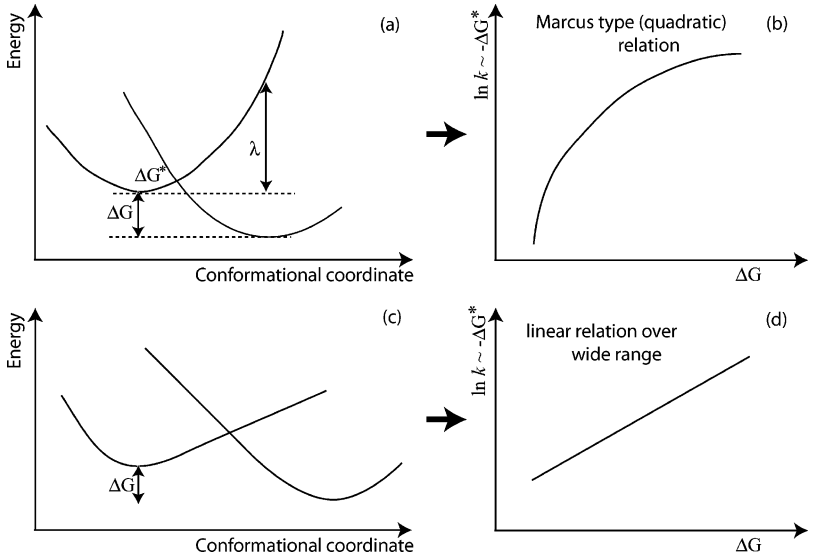

Figure 1. Schematic representation of the reaction rate dependence on the character of two energy surfaces. When the two energy surfaces are quadratic (a), the activation energy is related to the reaction free energy, ΔG, and the reorganization energy, λ, by eq 2, as in the theory of electron-transfer reactions. In this case, the reaction rate depends quadratically on the driving force ($-\Delta G$) (b). When the two energy surfaces are linear (c), the rate depends on the driving force linearly (d).

of ATP, ADP, and AMP, i.e., ATP + AMP ↔ ADP + ADP. Upon ligand binding the adenylate kinase undergoes a large conformational change.[18] Studies of adenylate kinase by normal-mode analysis have shown that the conformational change is well characterized by a few of the lowest frequency normal modes.[6] Our study focuses on the closure of the protein upon the binding of an inhibitor Ap_5A,[19] which is a bisubstrate analogue inhibitor that connects ATP and AMP by a fifth phosphate and mimics both substrates. Two conformations, open (Protein Data Bank ID code 4AKE)[18] and closed (Protein Data Bank ID code 1AKE),[19] of adenylate kinase are taken from PDB as the starting and ending points of the motion. Adenylate kinase consists of three domains: LID (residues 122−159), NMP_{bind} (30−59), and CORE (all other residues).[18]

Elastic Network Model. In this study, we use a coarse-grained model, the Tirion potential,[20] to represent the mechanical properties of the protein molecule. This potential is defined as follows: an interaction between two atoms, a and b, is taken to be the Hookean pairwise potential:

$$E(\mathbf{r}_a,\mathbf{r}_b) = \frac{C}{2}(|\mathbf{r}_{a,b}| - |\mathbf{r}^0_{a,b}|)^2 \qquad (5)$$

where $\mathbf{r}_a$ denotes the coordinate of atom a and $\mathbf{r}_{a,b} = \mathbf{r}_a - \mathbf{r}_b$. The zero superscript indicates the coordinate at the original conformation. The strength of the potential, C, is a constant assumed to be the same for all interacting pairs. The total potential energy of the system of N atoms is defined by

$$E = \sum_{\substack{a,b \\ |\mathbf{r}_{a,b}|<R}}^{N,N} E(\mathbf{r}_a,\mathbf{r}_b) \qquad (6)$$

where R is the cutoff parameter, so that the pair of interaction is limited to pairs of atoms separated by less than R. In this study, we use $R = 5$ Å, which has already been shown to be appropriate for normal mode studies of proteins.[21]

The spring constant C is a phenomenological constant assumed to be the same for all interacting pairs. The numerical value of the spring constant does not affect the eigenvectors obtained from normal-mode analysis; however, it determines the frequency of each normal mode, i.e., $(\text{frequency})^2 \propto C$. The spring constant needs to be calibrated to obtain the energy scale of the model. In this study, we estimated the spring constant by fitting C so that the averages of B factors from X-ray crystallography and normal-mode analysis are the same, using the relation B factor $\propto (\text{frequency})^{-2}$. Although the B factors in X-ray crystallography data and the atomic fluctuations in solution could be different because of crystal packing or crystal disorders, the B factors of the X-ray data would provide a reasonable estimation of the protein atomic fluctuations. Even if there is an error in the calibration, it does not affect our following discussion significantly, since only one parameter needs to be calibrated in our analysis and it affects only the energy scale. We should also note that effects of the solvent would be implicitly included in the model, since the energy scale is calibrated by the experimental data.

Although the Tirion potential was originally proposed for normal-mode analysis, we go beyond normal-mode analysis and use it to evaluate strain energy induced in the protein as the result of conformational change. This potential is crude but adequate to capture global mechanical property of molecules. In many respects, the Tirion potential is a variation of the Go model landscapes used in protein folding simulations.[22,23] It has been used by other groups[6,24−26] for normal-mode analyses to model protein dynamics. These studies suggest large-scale conformational transitions are dominated by low-frequency normal modes, largely determined by the low-resolution structure. Nevertheless, activation barriers and therefore rates cannot be discussed from a purely normal mode viewpoint.

Normal-Mode Analysis. Detailed descriptions of normal-mode analysis are in the standard literature.[27−29] Here we just define some quantities. Normal-mode analysis provides a set of normal-mode frequencies $\{\omega_n\}$, vectors $\{\mathbf{a}_n\}$, which are orthonormal, and normal mode coordinates $\{q_n\}$. We used the RTB method[30] for the diagonalization process of normal-mode analysis. This method allows calculation of the modes of large systems in very short times.[6,26]

Only a small portion of normal modes are relevant to the conformational change.[6] The overlap[31] is a measure of the similarity between the direction of the normal mode, $\mathbf{a}_n$, and the vector of the conformational change, $\mathbf{d}$, which is defined as $\cos\theta_n = \mathbf{d}\cdot\mathbf{a}_n/|\mathbf{d}|$. A value of 1 for this overlap would mean

that the directions of the normal mode n and the conformational change are identical.

Analysis of Conformational Change Path. To obtain the energy surface of the ligand unbound state, we first generate a sequence of structures along the conformational change path from the open form toward the closed form, using the iterative normal-mode analyses. For the structure at the iteration step i, denoted S_i, the unbound state energy of this structure, E_i^{unbound}, is calculated using eqs 5 and 6. The RMSD between the structure, S_i, and the open form, R^{open}, can be used as a reaction coordinate[10] for analyzing the energy surface.

In the present work, we also employed another set of reaction coordinates to describe the conformational changes. Adenylate kinase consists of three domains: LID (residues 122−159), NMP_{bind} (30−59), and CORE (all the other residues).[18] Conformational changes of adenylate kinase have been described as the domain motions of LID and NMP_{bind} domains relative to the CORE domain. Thus, polar rotation angles between the CORE domain and each of the LID and NMP_{bind} domains,[18] κ^{LID} and κ^{NMP}, can also be employed as other reaction coordinates. The closed form is taken as the origin, $(\kappa^{\text{LID}},\kappa^{\text{NMP}}) = (0°,0°)$. The coordinate of the open form is $(\kappa^{\text{LID}},\kappa^{\text{NMP}}) = (53°,45°)$.

Mapping between Two Reaction Coordinates. To evaluate the energy barrier for the conformational change, the two energy surfaces of the ligand-unbound and bound states need to be superimposed. The simplest idea is that there is direct switching of the potential function. However, directly implementing this naive method would not provide an accurate energy profile of large-scale conformational changes. Small differences in the local structure, in which we are not interested, induce large amounts of error in strain energy. Some of these differences in fact may be due to changes in refinement protocols and crystallization conditions for the two different conformations.[32] Combining this procedure with short minimization may solve the problem. We do not employ this method here. An alternative is to first generate two energy profiles, one from each stable form, and then superimpose them. However, with this method the two surfaces generally have different reaction coordinates. In our previous study,[10] we defined a mapping function of the RMSDs to the open and to the closed forms and superimposed the energy profiles from the open and closed forms.

In the present work, to describe the conformational change path, we employ another set of reaction coordinates, i.e., the two polar rotation angles between the CORE domain and each of the LID and NMP_{bind} domains, which can be used to define the mapping between the two energy profiles.

We consider the conformational transition from the open form to the closed form, i.e., the switching from the ligand unbound to the bound state. A sequence of structures that represents the conformational change path from the open to the closed form is denoted as, S_i, where i is the step number of the iterative procedure. For the structure S_i, the unbound state energy, E_i^{unbound}, is calculated as a strain from the original stable structure, S_1. However, the bound state energy, E_i^{bound}, cannot be directly calculated as discussed previously, because the paths from the closed and the open forms do not entirely overlap (see Results, Figure 5). Thus, to cover the same conformational space as the path from the open form, several conformational change paths are generated from the closed form, using several target structures. These target structures are taken from the conformational change path that is generated for studying the transition from the open form to the closed form. For each sampled structure, the ligand bound state energy, E_{bound}, and the reaction coordinates, $(\kappa^{\text{LID}},\kappa^{\text{NMP}})$, are calculated. The continuous two-dimensional energy surface of the closed state, $E_{\text{bound}}(\kappa^{\text{LID}},\kappa^{\text{NMP}})$, is obtained through interpolation of the sampled points. For a given structure, S_i, the polar rotation angles, $(\kappa_i^{\text{LID}},\kappa_i^{\text{NMP}})$, are calculated, and the bound state energy of this structure is given as $E_i^{\text{bound}} = E_{\text{bound}}(\kappa_i^{\text{LID}},\kappa_i^{\text{NMP}})$.

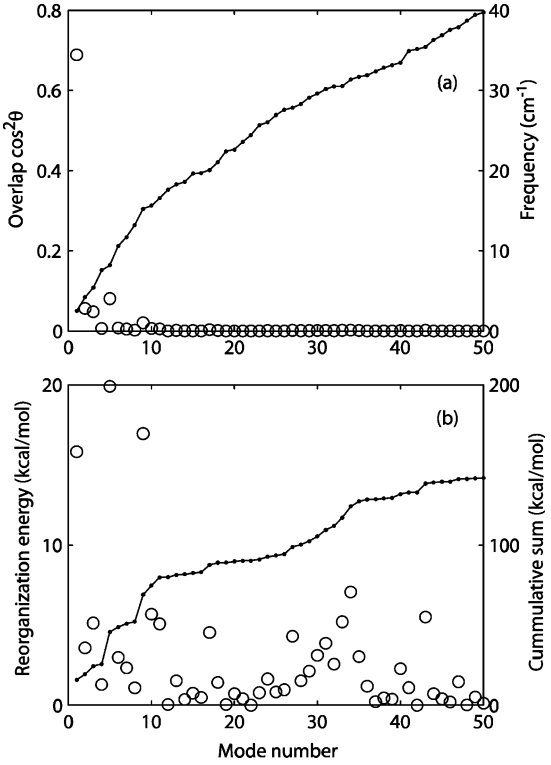

Figure 2. Estimation of the reorganization energy using simple normal-mode analysis. (a) Frequency (solid line) and degree of overlap (○) between the conformational change and each of calculated normal modes. The conformational change can be mostly described by a few low-frequency modes. (b) Contribution of each normal mode to the total reorganization energy, obtained from the linear elastic model, eq 3. Cumulative sum of contributions is shown by a solid line.

Results

Linear Elastic Model. Normal-mode analysis was performed for the open structure of adenylate kinase; the 50 lowest frequency modes were calculated. The Tirion potential depends on an arbitrary parameter, the spring constant C; thus, only relative frequencies are obtained from the calculation, and the numerical value needs to be calibrated from experimental data. The average B factor value, calculated from the experimental B factor of Cα atoms of the open form, is 38 Å^2. Thus, the value 3.5×10^{-1} kcal Å^{-2} is used to normalize the spring constant C for the following energy calculations. The scaled frequency is shown in Figure 2a. Figure 2a also shows the overlap between the conformational change and each normal mode. The lowest frequency normal mode (mode 1) gives the highest overlap, accounting for more than 65% of the total conformational change. In addition, small contributions from modes 2, 3, and 5 are observed. Other modes give only small contributions to the conformational change. Thus, the four highest overlap modes (1−3, 5) are most relevant to conformational change. Conformational change of adenylate kinase has been described as the domain motions of LID and NMP_{bind} domains relative to the CORE domain.[18] Normal mode 1 corresponds to the deformation of LID domain, and the other

higher frequency modes contribute more to the deformation of NMP_{bind} domain (result not shown).

From the overlap and frequency obtained by fitting to experimental data, we are able to calculate the contribution to the reorganization energy from each mode according to eq 3. The result is shown in Figure 2b. The lowest frequency mode (1) with the highest overlap gives a reorganization energy of about 15 kcal/mol. The second highest overlap mode (5) gives a higher reorganization energy, 20 kcal/mol, even though its overlap is lower than mode 1. The studies of X-ray crystal structure indicate that deformation of LID domain can be described by rigid-body movements while the NMP_{bind} domain movements are produced by a combination of shear motions.[33] The high reorganization energy for deformation of NMP_{bind} domain compared to the deformation of the LID domain is closely related to the different character of conformational changes, since the shear deformation requires stronger forces than the hinge bending deformation.

From the definition, eq 3, high overlap modes give large contributions to the reorganization energy. In addition, all things being equal, high-frequency modes give large contributions. Thus, higher frequency modes may contribute strongly, even though these modes are irrelevant to the conformational change in a strictly structural sense. For example, even though mode 34 contributes 0.2% to the conformational change (RMSD of 0.4 Å), its contribution for reorganization energy is large, 7 kcal/mol. However, higher frequency normal modes that do not contribute to the conformational change would be irrelevant for this analysis, and these contributions to the reorganization energy would probably not be reliable, since they are easily affected by small errors in the X-ray coordinates. If we take into account only the five modes with an overlap $> 1\%$ (RMSD of 0.7 Å), the estimated reorganization energy is still about 60 kcal/mol. Sanders II et al. have experimentally determined the standard binding free energy of MgATP and AMP as -5.2 and -4.6 kcal/mol, respectively.[34] The binding of the inhibitor Ap_5A would be stronger than these, since the Ap_5A is a combination of ATP and AMP. If we imagine the ligands are in rapid binding equilibrium, the effective free energy difference depends on the concentration of substrate. Varying the concentration between 1 mM and 1 μM affects the free energy difference in eq 1 by $4-8$ kcal/mol. If we use the energy difference of -3 kcal/mol as an example, the resulting activation energy is 14 kcal/mol.

From this linear elastic model, the contribution to the reorganization energy from mode 1 is about 15 kcal/mol. To check the validity of linear elastic model, we generate some deformed structures along mode 1 from the initial state and then calculate the energy of each structure. Figure 3 shows the obtained energy surface compared to the energy surface expected from the normal-mode frequency using $E = \omega^2 q^2/2$, where ω is the frequency of mode 1. The Tirion energy surface and the ideal harmonic description only agree in the vicinity of the energy minimum structure. The result indicates that even for the Tirion model, the energy surface is far from simple harmonic as the function of Cartesian coordinate of atoms. The apparent cause of the error is that a single set of normal mode vectors is not enough to represent the conformational change pathway. Examining the structural differences between the open and closed forms of adenylate kinase suggests that the conformational change resembles the bending of a rod. Bending is kinematically nonlinear in a Cartesian basis. However, a normal mode gives only the initial direction of the transformation, and if we follow a single mode too far along the direction of the conformational change, the protein can be distorted in the wrong way. This kinematic nonlinearity, well-known in macroscopic elastic theory, is the main shortcoming of the linear elastic model. To overcome this problem, in our previous study,[10] we employed an iterative procedure in which normal-mode analysis is repeatedly performed after each deformation in order to avoid inducing structural distortions due to nonlinearity. Such an iterative procedure has been shown to be beneficial for general structural modeling applications as a method to deform the structure considering the mechanical property of the molecule.[10,21] In the following, we discuss a nonlinear elastic model.

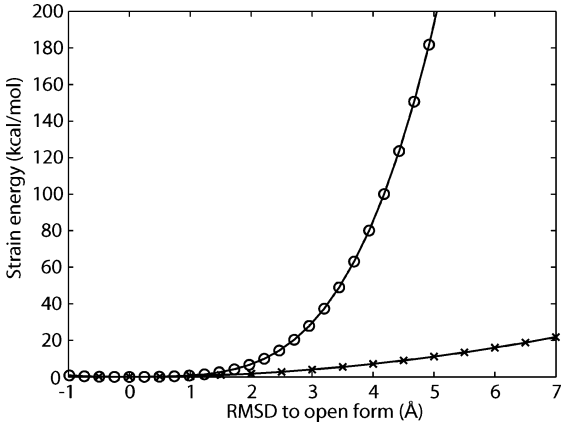

Figure 3. Comparison between energy surface, explicitly calculated, for the structures linearly deformed along mode 1, the lowest frequency mode, which is most relevant to the conformational change (○), and the energy surface modeled from the frequency of mode 1 at the initial state (×). RMSD = 5.9 Å corresponds to the projection of the final state on the normal mode coordinate 1. Explicitly calculated energy surface along mode 1 shows significant deviation from the harmonic surface.

Nonlinear Elastic Model. We generalize the model to include kinematic nonlinearity. We define the conformational change pathway in an iterative manner.[10,21] Now three conformational change paths from the open form to the closed forms are generated, using one, two, or three modes to deform the structure at each step. For the structures representing the conformational change paths, we calculated the strain energy using the spring network defined from the initial coordinate.

Figure 4 shows the resulting energy surface. Comparing with Figure 3, the energy surface along nonlinear conformational pathways gives lower energy. Until a certain point along the transformation, the energy surface is in good agreement with the energy surface that is expected by the frequency from normal-mode analysis. This agreement indicates that, though the harmonic approximation of the energy surface as a function of Cartesian coordinates is not accurate, the harmonic approximation of the energy surface as a function of a nonlinear reaction coordinate, RMSD for our model, can be satisfactory until a certain point.

The energy profile along the nonlinear deformation path starts to deviate from the harmonic curve around RMSD = 5 Å. To analyze this nonlinear behavior, we employ another reaction coordinate to describe the nonlinear conformational change path. For each structure, we examine the polar rotation angle between the CORE domain and each of the LID and NMP_{bind} domains.[18] Figure 5a shows the three nonlinear conformational paths, generated using 1, 2, or 3 modes, as functions of the polar angles of the LID and the NMP_{bind} domains. Figure 5a also shows a 2D energy surface interpolated from the strain energy of three conformational change paths. The obtained energy surface shows that the closure of the LID domain induces less strain energy than the closure of the NMP domain. For the nonlinear path

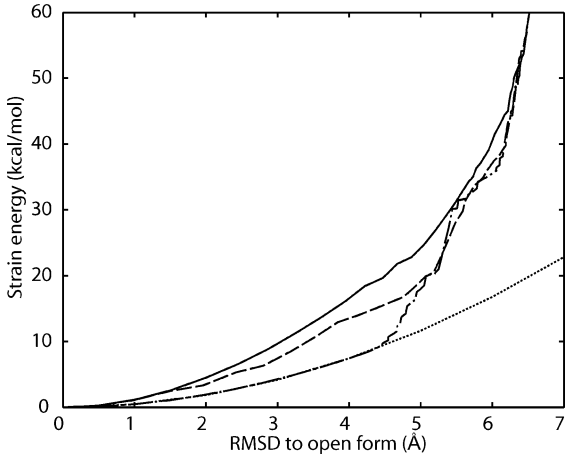

Figure 4. Energy surface along nonlinear conformational change path by iterative method. (a) Energy of structures along the path that was generated from the open form by iterative method using the highest overlap mode (dash−dot line), two highest modes (broken line), and three modes (solid line). The pure harmonic energy surface expected from the frequency of the lowest frequency mode is shown for comparison (dotted line).

generated with a single mode, comparison of the energy surfaces with the reaction coordinates RMSD and the polar rotation angles, the first harmonic phase (0 < RMSD < 5 Å in Figure 4) corresponds to deformation of the LID domain. Then the second phase (5 Å < RMSD), which deviates from the harmonic curve, corresponds to deformation of the NMP_{bind} domain. On the other hand, conformational change along the path made by three modes represents a concurrent deformation of the LID and NMP_{bind} domains; thus, the energy profile of the path using three modes is higher than the one using one mode. This observation is consistent with the deformation of NMP_{bind} domain being composed of the higher frequency modes, thus needing more strain energy. It also suggests that the LID domain preferably closes before the NMP_{bind} domain.

Analysis from the Closed Structure. A full understanding of the allosteric transition requires consideration of the product energy surface. Thus, we perform a similar analysis starting from the closed structure (PDB 1AKE[19]). The X-ray crystal structure of the closed form is a complex with the inhibitor Ap_5A.[19] The molecule closes upon ligand binding; thus, the closed form is energetically favorable in the ligand bound state. Our interest is in the elastic properties of the molecule in the ligand bound state. These properties are inherent in the shape of the closed form itself and the *B* factor from X-ray data. Thus, accounting for the ligand itself, is not necessary for the analysis, and it is not explicitly included in the following calculations.

The spring constant *C* of the Tirion potential is determined from the normal-mode analysis on the closed structure, independent of the open form. The crystal of the closed form contains two almost identical structures; however, their *B* factors are different by a factor of 2,[19] the average values of the fluctuation of Cα atoms being 27 and 49 $Å^2$. The difference would be due to the difference in the crystal packing.[19] Since there is no simple reason to prefer one *B* factor as the representative of the real atomic fluctuation, we have simply used the average for the calibration. Thus, $C = 7.3 \times 10^{-2}$ kcal $Å^{-2}$ is used for the following energy calculations. The choice of the calibration method could modulate the following result only slightly. We should note that the smaller coupling constant of the closed form, compared to that of the open form, does not mean the structural rigidity is weaker for the closed form since the rigidity of the Tirion potential also depends on the

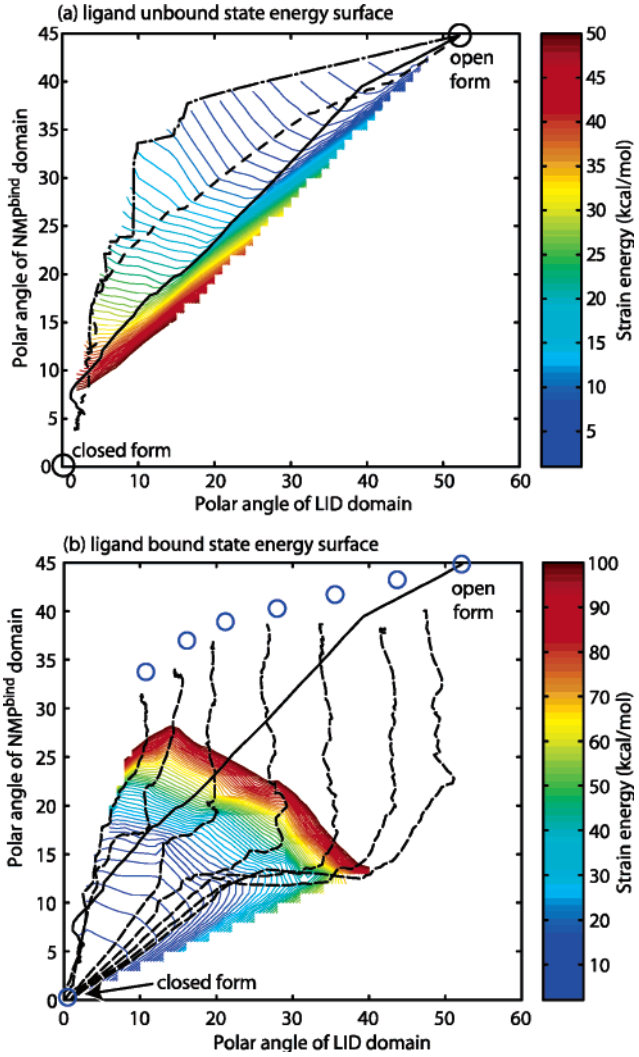

Figure 5. Energy surface with reaction coordinates polar rotation angle of LID and NMP_{bind} domain. The origin of polar axes (0°, 0°) is the closed form. (a) The energy surface of the ligand-unbound state. The nonlinear paths from open form by iteration with 3 modes (solid line), with 2 modes (broken line), and with 1 mode (dash−dot line) are projected in this angular coordinate space. The interpolated strain energy surface of the open state in superimposed as contour lines. (b) The energy surface of the ligand-bound state. Conformational change paths from the closed form toward different target structures are projected in the angular coordinate space (broken lines). Targets used to generate these paths were the 0th, 10th, ..., and 60th structures along the path from the open form that were generated using 1 mode, shown in (○). These paths are used to obtain the energy surface of the ligand-bound state, which are shown as contour lines. The nonlinear path from the open form toward the closed form by iteration with 3 modes is shown by a solid line.

number of atom−atom interactions. The *B* factor from normal-mode analysis with $C = 1$ gives a smaller value for the closed form than for the open form. This indicates that the closed form has a denser network than the open form.

Superimposed Energy Surfaces. To obtain the overall energy surface of the conformational change, the energy surfaces from the open and closed forms are superimposed. The energy surface of the closed state as a function of the polar rotation angles of the LID and NMP_{bind} domains is shown in Figure 5b. Here, we focus on the conformational change path generated using three modes. From the energy surfaces shown in Figure 5, the ligand-unbound and ligand-bound state energy profiles along the conformational change paths are obtained. Superimposed strain energy profiles are shown in Figure 6, using the

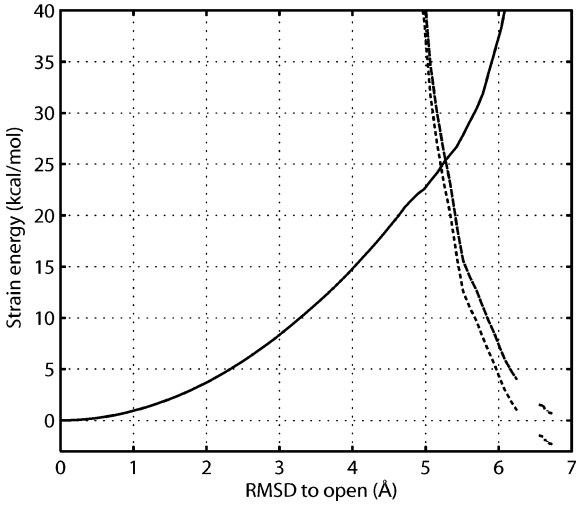

Figure 6. Superposition of energy profiles of the ligand-unbound and bound states along a representative conformational change path, which is obtained from the 2-dimensional energy surfaces (Figure 5). The energy profile of the open state is indicated by a solid line, the closed form with free energy change $\Delta G_{\text{react}} = 0$ kcal/mol by a broken line, and $\Delta G_{\text{react}} = -3$ kcal/mol by a dotted line.

RMSD from the open form as the reaction coordinate. The difference in minimum energy of the two energy profiles, ΔG_{react}, was varied from 0 to -3 kcal/mol. From the crossing point of the two energy profiles, we obtained an activation energy of ~25 kcal/mol, which slightly depends on the driving force ($-\Delta G_{\text{react}}$).

The energy barrier obtained here is higher than in our previous study (~20 kcal/mol).[10] The difference arises from the difference of the structures paired at the crossing point. With the previous mapping method based on RMSD reaction coordinate, the pair of structures from open and closed forms has RMSD of ~2.2 Å. In the current procedure with the 2-dimensional angles reaction coordinates, the pair has RMSD of ~1.9 Å. Thus, the paired structures coincide slightly more closely with this new mapping method. The slightly higher energy barrier results from minor arrangement of the structure. With a larger number of reaction coordinates, the mapped structures can coincidence more closely. However, an attempt to deform structures to have exactly the same conformation would not have meaning. There is some uncertainty in the position of the atoms in X-ray structure. The atomic displacements observed in the paired structures are within the range of the thermal fluctuations. Comparing the RMSD based with the 2-dimensional angles based mapping procedures, we observed the residue RMSD between the paired structures is distributed more evenly by the 2-dimensional procedure (results not shown), which ensures that the main characteristics of the conformational changes have been fully taken into account.

The activation energy barrier observed here (~25 kcal/mol) is very high compare to the value estimated in the linear elastic model (~15 kcal/mol). We estimate the energy barrier from the linear elastic model by assuming a perfectly harmonic energy surface, eq 3. However, as we have seen in Figure 4, the energy surface does not remain quadratic, even after the nonlinearity of conformational change is taken into account by the iterative procedure, and thus the actual energy barrier is higher. In the linear elastic model, we also assumed that the energy surfaces of the two states have the same curvature, and we estimated the energy barrier from the frequency of the open form. However, the deformation from the closed form needs much more energy (see Figure 5b), and the crossing point is 2 times higher. Some previous studies on the protein electron-transfer reactions[35,36] have used the linear elastic models; however, the inaccuracy due to the nonlinearity would be small for these results, since the change of conformation resulting from electron transfer is very small compared to the changes discussed in the allostery.

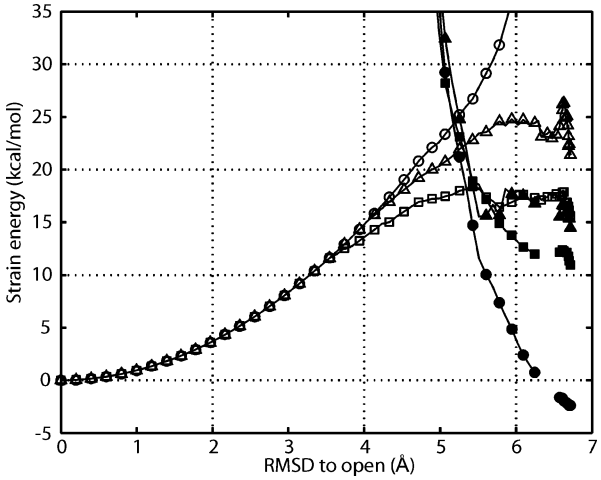

Figure 7. Energy surface with cracking effects. Calculations of energy profiles from the nonlinear elastic model without cracking are marked (○), with cracking and surface tension $\sigma = 1$ are (△), and with cracking for $\sigma = 0.5$ kcal/mol are (□). Energies of the ligand-unbound state are shown by open markers, and the ligand bound state are shown by filled markers. Free energy change of $\Delta G_{\text{react}} = -3$ kcal/mol is employed in this figure as a representative. The cracking effect lowers the energy barrier. The energy surface of the ligand bound states with low surface tension has higher energy than one without cracking, since some residues are partially unfolded. Actual conformational change would involve a refolding process, i.e., shift from the energy profile with cracking to the energy profile without cracking.

Partial Unfolding Lowers the Activation Barrier. The energy barrier obtained from these studies is very high, even higher than the total stability of the protein. In our previous study, following the conformational change pathway obtained by the iterative method, we analyzed which part of protein is under high strain energy.[10] Strain energy of each residue is defined as the sum of atomic strain energies, which is half of the elastic energy defined by eq 5. Strain energy in the molecule due to conformational deformation was found to be very localized. The observations that some particular residues are under high strain energy led us to hypothesize that these highly strained residues *crack*, i.e., unfold partially, during conformational change.[10] To include this possibility, we consider a model in which residues are allowed to partially unfold (see Cracking Model in Theory and Models). The unfolding free energy, ΔG_{fold}, of adenylate kinase from *E. coli* is reported to be ~10 kcal/mol for urea denaturation.[37] Under the assumption that unfolding energy of one residue is equal to the total unfolding energy divided by the number of residues, $N_{\text{res}} = 214$, we used the cracking threshold of $\Delta G_{\text{unbound}}^{\text{residue}} = \Delta G_{\text{fold}}/N_{\text{res}} \sim 0.05$ kcal/mol. The surface tension σ of the cracking region was tested in the range of 0.5−1.5 kcal/mol.

The resulting energy surface along the allosteric conformational change is shown in Figure 7. Obviously, the partial unfolding model gives a lower energy barrier. The extent of cracking strongly depends on the surface cost σ. Note that the energy of the ligand-bound state is higher when there is cracking. For this energy calculation, a part of the protein is assumed to remain unfolded when it switches from the unbound state to the bound state, thus having a higher energy than the native folded state. In a real situation, once the binding occurs, the

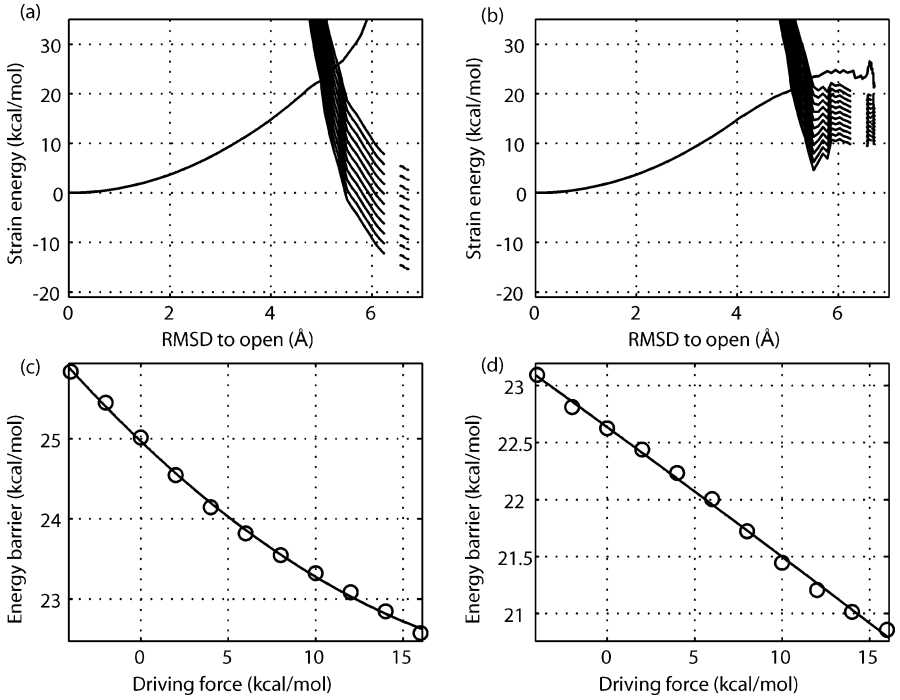

Figure 8. Transition state barrier dependence on the reaction driving force. The transition state barrier, ΔG^*, vs the reaction driving force, $-\Delta G_{react}$, both without cracking (a) and with cracking (b) are shown. We considered driving forces ranging from -4 to 14 kcal/mol. The corresponding energy surfaces at the different driving forces ($-\Delta G_{react}$) without cracking (c) and with cracking (d) are also shown. A quadratic curvature is observed for the fully elastic model without cracking. Including the cracking effect makes the barrier dependence on driving force more linear.

protein would refold, i.e., shift from the energy surface with cracking to the one without cracking, thus lowering the energy. The energy changes due to such refolding transition are not shown explicitly. One interesting observation is that cracking leads to an energy surface which is approximately a linear function of the deformation, rather than following the quadratic dependence of the elastic regime. Such linear relations have also been invoked to explain the efficiency of motor proteins by Oster et al.[38] The cracking model suggests the linear behavior may be much more general in protein conformational transitions.

Effect of Cracking on the Conformational Change Rate. The qualitative difference between the energy surface with or without cracking effects, i.e., quadratic or linear, is the dependence of kinetics on the driving force for binding. Without unfolding, the free energy profiles of reactant and product states are quadratic as a function of a reaction coordinate (Figure 1a). In such a case, the activation free energy, ΔG^*, can be expressed by the reorganization energy, λ, and the reaction free energy, ΔG, as eq 2. The consequence of this relation is a characteristic quadratic dependence of the log of the kinetic rate on the driving force, $-\Delta G$ (Figure 1b). On the other hand, when unfolding or cracking is allowed, the free energy surfaces become locally linear. When the free energy profiles of two states are linear as a function of a reaction coordinate (Figure 1c), the energy barrier depends linearly on the reaction coordinate (Figure 1d). This qualitative difference can be tested. We examined the dependence of the activation barrier on the driving force in our model. Figure 8 shows how the transition state barrier depends on the reaction driving force. Here we vary the driving force from -4 to 14 kcal/mol. The characteristic curvature of parabolas is observed for a fully elastic model, while inclusion of cracking makes the dependence more nearly linear.

More importantly, the cracking model allows residues that are folded in both stable states to become unfolded in the transition state. Thus, a dependence of the reaction rate on folding stability change is predicted: simultaneously lowering the stability of both conformations without changing their relative stability will speed up the reaction. Using site directed mutagenesis, one can determine the probability of individual residues to remain structured or to crack during the transition, as in folding Φ value analysis.[39] Evidence for cracking can also be gleaned using the global effects of denaturants, such as urea, on conformational change kinetics. Denaturant will enhance the local unfolding and therefore should lower the barrier height. Such anomalous activation of enzymes by adding low concentrations of denaturant has been observed in this and other systems.[40−42] Such a denaturing effect has also been observed in thermophilic organisms under low temperatures.[43] These activation effects are not monotonic. At higher concentration, as anyone would expect, denaturation reduces the activity. However, at low levels of denaturant the activity does indeed increase in accord with our model. Under the assumption that the conformational change is the rate-determining step, we could relate the enhancement of the activity to the lowering of the energy barrier. The increase in activity of adenylate kinase was studied experimentally by adding denaturant.[40] The activity was initially enhanced by 1.25-fold in 0.2 M (molar concentration) urea, compared to in the absence of urea, and reached a maximum (1.6-fold enhancement) by 1 M of urea, which corresponds to a $\partial\Delta G^*/\partial$[urea] in the range of 0.2−0.7 kcal/(mol M).

We have computed the analogous slope for our theoretical model of the conformational change. In the present model, only the surface tension σ is an arbitrary parameter in these analyses, and we have tested $\sigma = 0.5$, 1, and 1.5 kcal/mol. All other parameters are taken from experimental data. Figure 9 shows the activation free energy, ΔG^*, dependence on ΔG_{fold}. A driving force of $\Delta G_{react} = -3$ kcal/mol is used. The data are fitted by a hyperbolic function. The choice of model (e.g., exponential or hyperbolic) for the fitting needs further investigations. The total stability of the adenylate kinase is 10 kcal/mol.[37] The slope $\alpha = \partial\Delta G^*/\partial\Delta G_{fold}$ at $\Delta G_{fold} = 10$ is estimated to be

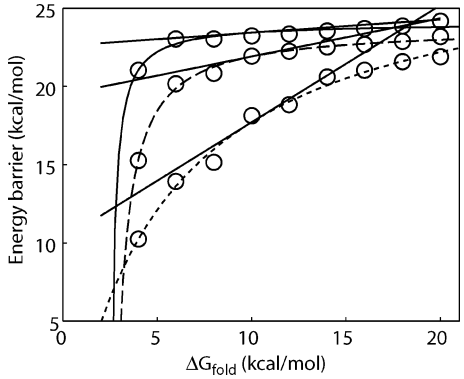

Figure 9. Transition state barrier dependence on the cracking threshold. This figure shows how the transition state barrier, ΔG^*, depends on the protein stability, ΔG_{fold}. A driving force of $\Delta G_{react} = -3$ kcal/mol is used. Three values of surface tension, $\sigma = 1.5$, 1, or 0.5 kcal/mol, are tested. For each $\sigma = 1.5$ kcal/mol (solid line), $\sigma = 1$ kcal/mol (broken line), and $\sigma = 0.5$ kcal/mol (dotted line), the data are fitted hyperbolically to $\partial\Delta G^* = -4.9/(\Delta G_{fold} - 2.4) + 24$, $\partial\Delta G^* = -14/(\Delta G_{fold} - 2.3) + 24$, and $\partial\Delta G^* = -167/(\Delta G_{fold} + 4.9) + 28$, respectively. From the slope of the line, the slope $\alpha = \partial\Delta G^*/\partial\Delta G_{fold}$ at $\Delta G_{fold} = 10$ kcal/mol is estimated as 0.084 for $\sigma = 1.5$ kcal/mol, 0.24 for $\sigma = 1$ kcal/mol, and 0.75 for $\sigma = 0.5$ kcal/mol. These are used for the estimations of $\partial\Delta G^*/\partial$[urea] in the main text.

0.084 with $\sigma = 1.5$ kcal/mol, 0.24 with $\sigma = 1$ kcal/mol, and 0.75 with $\sigma = 0.5$ kcal/mol. The experimentally determined urea dependence of the stability $m = \partial\Delta G_{fold}/\partial$[urea] = 2.9 kcal/(mol M);[37] here M is the molar concentration of urea. Combining these, the urea dependence of the transition barrier, $\partial\Delta G^*/\partial$[urea], is about 0.24 kcal/(mol M) if $\sigma = 1.5$ kcal/mol, 0.69 kcal/(mol M) if $\sigma = 1$, and about 2.1 kcal/(mol M) if $\sigma = 0.5$. These results are remarkably consistent with the experimental speedup described above.

The lowering of the energy barrier from the cracking varies depending on the stability of the protein ΔG_{fold}. Therefore, the cracking effect on the rate is large when the stability of the protein, ΔG_{fold}, is originally low, i.e., the molecule is fragile. On the other hand, if the threshold is high or the molecule is rigid, the effect of cracking on the rate will be weak or none. In the range of variables tested, adenylate kinase seems to be just at the intermediate between the two limits, neither too fragile nor too rigid. This would suggest that Nature has optimized the molecule so that the energy barrier is lowered by the cracking mechanism, while structural integrity is kept for proper function. Such a possibility could be tested further through a survey of several proteins.

Conclusion

In this study, we revisited our previously proposed model to describe the energy landscape of protein conformational changes[10] and made several new advances in the proposed model. First, we discussed the theoretical aspect of our model which describes the binding coupled conformational transition as a switching between the two separated energy surfaces. This approximation is valid when the conformational transition is slow compared the substrate binding processes. The conformational change of the adenylate kinase was discussed using polar rotation angles of mobile domains as reaction coordinates. The results indicated that the LID domain is more flexible than the NMP_{bind} domain, and it could close preferably upon ligand binding. A new model for the partial unfolding, or cracking, during the conformational change transition was also proposed. We improved our model compared to the previous one by including the cooperativity of the partial unfolding as an analogy to the nucleation process. The comparisons to the experimental data of activation of the adenylate kinase showed remarkable agreement. However, direct measurements of the conformational change kinetics, not as a composite with other chemical steps, as a function of denaturant is needed to test our model more completely. While the conformational change step has been kinetically isolated in the related systems of CSK and PKA,[44,45] the denaturant dependence has yet to be studied. Although the present model is quite simple, and can be refined using models containing more details, the agreement between theory and experiment shows the potential of the present approach for quantitatively understanding the underlying mechanisms governing allosteric motions.

Acknowledgment. We acknowledge Y. H. Sanejouand and F. Tama for making the program package RTB available to us. This work was supported by NSF Grants PHY-0216576, 0225630, and MCB-0084797 to J.N.O. The authors thank the W.M. Keck Foundation for computational support.

References and Notes

(1) Gerstein, M.; Krebs, W. *Nucleic Acids Res.* **1998**, *26*, 4280.
(2) Kim, M. K.; Jernigan, R. L.; Chirikjian, G. S. *Biophys. J.* **2002**, *83*, 1620.
(3) Schlitter, J.; Engels, M.; Kruger, P. *J. Mol. Graph.* **1994**, *12*, 84.
(4) Guilbert, C.; Perahia, D.; Mouawad, L. *Comput. Phys. Commun.* **1995**, *91*, 263.
(5) McCammon, J. A.; Gelin, B. R.; Karplus, M.; Wolynes, P. G. *Nature (London)* **1976**, *262*, 325.
(6) Tama, F.; Sanejouand, Y. H. *Protein Eng.* **2001**, *14*, 1.
(7) Mouawad, L.; Perahia, D. *J. Mol. Biol.* **1996**, *258*, 393.
(8) Tama, F.; Brooks, C. L., III *J. Mol. Biol.* **2002**, *318*, 733.
(9) Xu, C.; Tobi, D.; Bahar, I. *J. Mol. Biol.* **2003**, *333*, 153.
(10) Miyashita, O.; Onuchic, J. N.; Wolynes, P. G. *Proc. Natl. Acad. Sci. U.S.A.* **2003**, *100*, 12570.
(11) Levich, V. G.; Dogonadze, R. R. *Dokl. Akad. Nauk SSSR Ser. Fiz. Khim.* **1959**, *124*, 123.
(12) Marcus, R. A.; Sutin, N. *Biochim. Biophys. Acta* **1985**, *811*, 265.
(13) Volkman, B. F.; Lipson, D.; Wemmer, D. E.; Kern, D. *Science* **2001**, *291*, 2429.
(14) Agmon, N.; Hopfield, J. J. *J. Chem. Phys.* **1983**, *78*, 6947.
(15) Goldstein, H. *Classical Mechanics*, 2nd ed.; Addison-Wesley Pub. Co.: Reading, MA, 1980.
(16) Basu, G.; Kitao, A.; Kuki, A.; Go, N. *J. Phys. Chem. B* **1998**, *102*, 2076.
(17) Munoz, V.; Eaton, W. A. *Proc. Natl. Acad. Sci. U.S.A.* **1999**, *96*, 11311.
(18) Muller, C. W.; Schlauderer, G. J.; Reinstein, J.; Schulz, G. E. *Structure* **1996**, *4*, 147.
(19) Muller, C. W.; Schulz, G. E. *J. Mol. Biol.* **1992**, *224*, 159.
(20) Tirion, M. M. *Phys. Rev. Lett.* **1996**, *77*, 1905.
(21) Tama, F.; Miyashita, O.; Brooks, C. L., III *J. Mol. Biol.* **2004**, *337*, 985.
(22) Go, N. *Annu. Rev. Biophys. Bioeng.* **1983**, *12*, 183.
(23) Clementi, C.; Nymeyer, H.; Onuchic, J. N. *J. Mol. Biol.* **2000**, *298*, 937.
(24) Atilgan, A. R.; Durell, S. R.; Jernigan, R. L.; Demirel, M. C.; Keskin, O.; Bahar, I. *Biophys. J.* **2001**, *80*, 505.
(25) Doruker, P.; Jernigan, R. L.; Bahar, I. *J. Comput. Chem.* **2002**, *23*, 119.
(26) Tama, F.; Valle, M.; Frank, J.; Brooks, C. L., III *Proc. Natl. Acad. Sci. U.S.A.* **2003**, *100*, 9319.
(27) Go, N.; Noguti, T.; Nishikawa, T. *Proc. Natl. Acad. Sci. U.S.A.* **1983**, *80*, 3696.
(28) Brooks, B. R.; Karplus, M. *Proc. Natl. Acad. Sci. U.S.A.* **1983**, *80*, 6571.
(29) Case, D. A. *Curr. Opin. Struct. Biol.* **1994**, *4*, 285.
(30) Tama, F.; Gadea, F. X.; Marques, O.; Sanejouand, Y. H. *Proteins Struct. Funct. Genet.* **2000**, *41*, 1.
(31) Marques, O.; Sanejouand, Y. H. *Proteins* **1995**, *23*, 557.
(32) DePristo, M. A.; de Bakker, P. I.; Blundell, T. L. *Structure* **2004**, *12*, 831.
(33) Schulz, G. E. *Faraday Discuss.* **1992**, 85.
(34) Sanders, C. R., II; Tian, G. C.; Tsai, M. D. *Biochemistry* **1989**, *28*, 9028.
(35) Basu, G.; Kitao, A.; Kuki, A.; Go, N. *J. Phys. Chem. B* **1998**, *102*, 2085.

(36) Miyashita, O.; Go, N. *J. Phys. Chem. B* **1999**, *103*, 562.
(37) Burlacu-Miron, S.; Perrier, V.; Gilles, A. M.; Pistotnik, E.; Craescu, C. T. *J. Biol. Chem.* **1998**, *273*, 19102.
(38) Bustamante, C.; Keller, D.; Oster, G. *Acc. Chem. Res.* **2001**, *34*, 412.
(39) Fersht, A. *Structure and Mechanism in Protein Science: A Guide to Enzyme Catalysis and Protein Folding*; W.H. Freeman: New York, 1999.
(40) Zhang, H. J.; Sheng, X. R.; Pan, X. M.; Zhou, J. M. *Biochem. Biophys. Res. Commun.* **1997**, *238*, 382.
(41) Fan, Y. X.; Ju, M.; Zhou, J. M.; Tsou, C. L. *Biochim. Biophys. Acta* **1995**, *1252*, 151.
(42) Das, M.; Dasgupta, D. *FEBS Lett.* **1998**, *427*, 337.
(43) Zoldak, G.; Sut'ak, R.; Antalik, M.; Sprinzl, M.; Sedlak, E. *Eur. J. Biochem.* **2003**, *270*, 4887.
(44) Adams, J. A. *Chem. Rev.* **2001**, *101*, 2271.
(45) Hamuro, Y.; Wong, L.; Shaffer, J.; Kim, J. S.; Stranz, D. D.; Jennings, P. A.; Woods, V. L., Jr.; Adams, J. A. *J. Mol. Biol.* **2002**, *323*, 871.